JURNAL LOCUS: Penelitian & Pengabdian
Volume 5 No. 11 November 2026, pp 10455-10465
E-ISSN 2829-7334
DOI: 10.58344/locus.v5i11.6541

Performance Evaluation of A Dynamic Voltage Restorer for Voltage Sag Mitigation in a 20-kV Feeder Supplying a 555-kVA Connected Dolomite Industrial Installation

Hadroh Ahmad Budiman* , Syamsir Abduh
Institut Teknologi PLN, Indonesia
Email : hadroh2410716@itpln.ac.id* , syamsir@itpln.ac.id

Keywords:
Dynamic Voltage Restorer; Voltage Sag; Power Quality; Industrial Load; Distribution System.

This is an open access article under the CC BY-SA license.

Copyright © 2026 by Hadroh Ahmad Budiman, Syamsir Abduh. Published by Riviera Publishing

ABSTRACT

Voltage sags can disrupt industrial processes by reducing motor torque, causing contactor dropout, and triggering malfunctions in sensitive control systems and power electronic equipment. This study evaluated the performance of a dynamic voltage restorer (DVR) in mitigating voltage sags on a 20-kV distribution feeder supplying a dolomite processing facility with a connected load capacity of 555 kVA. The MATLAB/Simulink model incorporated a 630-kVA, 20-kV/400-V distribution transformer and an operating point derived from customer automatic meter reading (AMR) data, comprising an active power of 416.8 kW, reactive power of 124.0 kVAr, apparent power of 433.6 kVA, and a power factor of 0.947. A balanced three-phase voltage sag lasting 0.10 s was simulated, and the load voltage was assessed under uncompensated and DVR-compensated conditions. The voltage sag reduced the line-to-line load voltage from 406.57 V to 345.35 V, corresponding to a sag depth of 15.06% and a retained voltage of 84.94%. Following DVR activation, the load voltage increased to 404.82 V. The DVR compensated for 59.47 V of the 61.22-V voltage reduction, achieving a voltage restoration level of 99.57% relative to the pre-sag voltage, a sag mitigation effectiveness of 97.15%, and a residual voltage error of 0.43%. These findings demonstrated that series voltage injection effectively restored the industrial load voltage to near its pre-sag level, providing a technical basis for evaluating DVR applications in utility-supplied medium-voltage distribution systems serving industrial facilities.

INTRODUCTION

Industrial facilities increasingly rely on induction motors, contactors, adjustable-speed drives, automated control systems, and power electronic interfaces. Although these technologies enhance operational efficiency and process performance, they also increase the dependence of industrial operations on the quality and stability of the supplied voltage (Wu et al., 2021). Short-duration reductions in root-mean-square (RMS) voltage can reduce motor torque, cause contactor dropout, trigger drive protection systems, or reset control circuits, potentially transforming temporary electrical disturbances into production interruptions and economic losses (Bollen, 2000; Dugan et al., 2012; Fuchs & Masoum, 2023; Institute of Electrical and Electronics Engineers [IEEE], 2023; Pilipenko, 2025; Tang et al., 2022).

Voltage sags are characterized primarily by the magnitude of the retained RMS voltage and the duration of the voltage reduction. Their severity depends on the retained voltage magnitude, event duration, phase characteristics, and equipment sensitivity rather than solely on the magnitude of the voltage reduction (Bollen, 2000; Dugan et al., 2012). Consistent RMS

measurement windows are essential because switching transients and fault inception disturbances may distort the estimated sag magnitude when included in the measurement interval (International Electrotechnical Commission [IEC], 2021). For three-phase industrial loads, the line-to-line voltage measured at the load terminals provides a relevant indicator of the voltage supplied to connected equipment.

A dynamic voltage restorer (DVR) is a series-connected power electronic compensator that injects a controlled voltage to maintain the load-side voltage near its reference value during source-side voltage sags. Previous medium-voltage experimental investigations established the practical feasibility of DVR operation (Nielsen et al., 2004), while subsequent reviews examined converter topologies, operating modes, compensation strategies, and control techniques (Moghassemi & Padmanaban, 2020; Prasad et al., 2022; Soomro et al., 2021). More recent studies have focused on advanced intelligent and nonlinear control strategies, as well as improvements in converter configurations and system performance (Abdelaal et al., 2024; Abdul Rahman et al., 2024; Liu et al., 2024; Mattar et al., 2024; Mbuli, 2023; Tan et al., 2023). Despite these technological advancements, application-specific evaluations based on actual utility operating conditions remain important for assessing DVR performance in industrial distribution systems (Siddique et al., 2024).

This study addressed this need by evaluating a dolomite processing facility supplied through a 20-kV distribution feeder operated by PT PLN (Persero), Indonesia's state-owned electricity utility. The facility had a connected load capacity of 555 kVA, while the evaluated operating point, obtained from automatic meter reading (AMR) data, corresponded to an apparent power demand of 433.6 kVA. The simulation model incorporated a 630-kVA distribution transformer. Accordingly, the connected load capacity, measured operating demand, and transformer rated capacity were distinguished as separate technical parameters throughout the analysis.

The novelty of this study lies in its application-oriented evaluation framework based on utility-specific operating conditions rather than the development of a new DVR topology or control algorithm. The study makes three principal contributions. First, it establishes a simulation-based evaluation model using field-derived AMR data from a facility with a connected capacity of 555 kVA and an operating demand of 433.6 kVA. Second, it quantitatively assesses DVR performance using load-voltage profiles, voltage compensation requirements, restored voltage magnitude, voltage recovery, sag mitigation effectiveness, and residual voltage error. Third, it provides an application-specific technical reference for assessing the potential implementation of DVR technology on a utility-operated 20-kV distribution feeder supplying an industrial load.

Accordingly, this study aimed to quantify the severity of voltage sags at the selected industrial installation, evaluate the compensation performance of an equivalent series voltage injection DVR model, and interpret the findings in relation to established DVR principles and comparable industrial applications. The investigation was limited to a simulation-based performance assessment and did not involve the development or comparative optimization of DVR control algorithms or converter topologies. The findings are expected to provide a reproducible evaluation approach for utility engineers, support preliminary technical feasibility assessments of DVR applications in similar medium-voltage industrial distribution systems,

and establish a reference case for future experimental validation and smart grid integration research.

METHOD

System Description and Simulation Model

Industrial Load and AMR Data

The study examined a dolomite processing facility with a connected load capacity of 555 kVA. Customer automatic meter reading (AMR) data were used to establish the actual operating conditions rather than reconstruct a voltage sag event. The metering system had a current transformer (CT) ratio of 20/5, a potential transformer (PT) ratio of 20,000/100, and a meter constant of 1, resulting in a meter multiplication factor of 800. The selected operating point comprised a line-to-line grid voltage of 20.634 kV, active power of 416.8 kW, reactive power of 124.0 kVAr, apparent power of 433.6 kVA, a power factor of 0.947, and a frequency of 50 Hz. Based on the nominal transformer voltage ratio, the estimated low-voltage-side voltage was 412.68 V. The simulation reference voltage was subsequently established using the root-mean-square (RMS) voltage measured at the stabilized load terminals.

Table 1. Actual operating data and installation parameters

Parameter	Value
Connected installation capacity	555 kVA
AMR grid voltage (line-to-line)	20.634 kV
Active power	416.8 kW
Reactive power	124.0 kVAr
Apparent power	433.6 kVA
Power factor	0.947
Frequency	50 Hz
Installation utilization	78.13 percent
CT ratio / PT ratio	4 / 200
Meter constant / multiplication factor	1 / 800

The operating demand of 433.6 kVA represented 78.13% of the facility's connected load capacity of 555 kVA. This percentage indicated the utilization of the connected capacity rather than the transformer loading.

Distribution Source and Transformer Model

The three-phase power source was configured with a line-to-line voltage of 20.634 kV and a frequency of 50 Hz. A short-circuit capacity of 250 MVA and an reactance-to-resistance (X/R) ratio of 10 were used to determine an equivalent source resistance of 0.1695 Ω and an inductance of 0.0054 H, thereby accounting for source impedance rather than assuming an ideal voltage source. A 630-kVA, 20-kV/400-V distribution transformer was modeled to connect the medium-voltage and low-voltage networks. Each winding was assigned a resistance of 0.002 per unit (pu) and a leakage reactance of 0.030 pu, resulting in an equivalent transformer impedance of approximately 6.01%.

The investigated dolomite processing facility had a connected load capacity of 555 kVA, while the operating demand obtained from automatic meter reading (AMR) data was 433.6 kVA. The distribution transformer incorporated into the simulation model had a rated capacity of 630 kVA. Accordingly, the transformer operated at approximately 68.83% of its rated capacity under the evaluated conditions.

Voltage Sag Scenario

The voltage sag scenario (Sag-1) was simulated by applying a balanced three-phase-to-ground fault at the low-voltage load bus from 0.10 to 0.20 s. This configuration established a controlled, balanced voltage sag for comparing load-terminal voltages under uncompensated and dynamic voltage restorer (DVR)-compensated conditions. The fault duration was 0.10 s, equivalent to five cycles at 50 Hz. The fault resistance and ground resistance were set to 0.03 Ω and 0.001 Ω, respectively, with a total simulation duration of 0.30 s. Root-mean-square (RMS) voltages under normal operating conditions were evaluated over 0.05–0.09 s, while voltages during Sag-1 were evaluated over 0.12–0.18 s. These measurement intervals excluded fault inception and clearing transients to ensure consistent voltage assessment. All voltage measurements were obtained from the same load-terminal measurement point.

Equivalent DVR Model

The DVR was modeled using an equivalent series voltage injection configuration comprising three Controlled Voltage Source blocks. Sinusoidal reference signals at 50 Hz were applied with phase angles of 0°, −120°, and +120° for phases A, B, and C, respectively. Series voltage injection was activated between 0.10 and 0.20 s, with a reference amplitude of 58 V peak per phase, corresponding to approximately 41.01 V RMS per phase. The model represented the electrical effects of series voltage compensation without explicitly modeling the DC link, voltage-source inverter, pulse-width modulation (PWM) stage, output filter, or injection transformer as separate switching subsystems.

Table 2. Simulation system, transformer, fault, and DVR parameters

Parameter	Value
Source operating voltage / frequency	20.634 kV line-to-line / 50 Hz
Short-circuit level / X/R	250 MVA / 10
Equivalent source R / L	0.1695 ohm / 0.0054 H
Transformer rating	630 kVA, 20 kV/400 V
Winding R1 = R2	0.002 pu
Leakage L1 = L2	0.030 pu
Equivalent impedance / loading	6.01 percent / 68.83 percent
Fault configuration	Balanced three-phase-to-ground
Fault R / ground R	0.03 ohm / 0.001 ohm
Fault interval / duration	0.10–0.20 s / 0.10 s
Measurement windows	Normal: 0.05–0.09 s; sag: 0.12–0.18 s
DVR injection reference	58 V peak/phase = 41.01 V rms/phase
Injection angles / frequency	0, −120, +120 degrees / 50 Hz

The complete series-injection arrangement is shown in Figure 1. The same source, transformer, load, fault, and measurement parameters were retained in the uncompensated and compensated simulations; DVR activation was the only intentional difference.

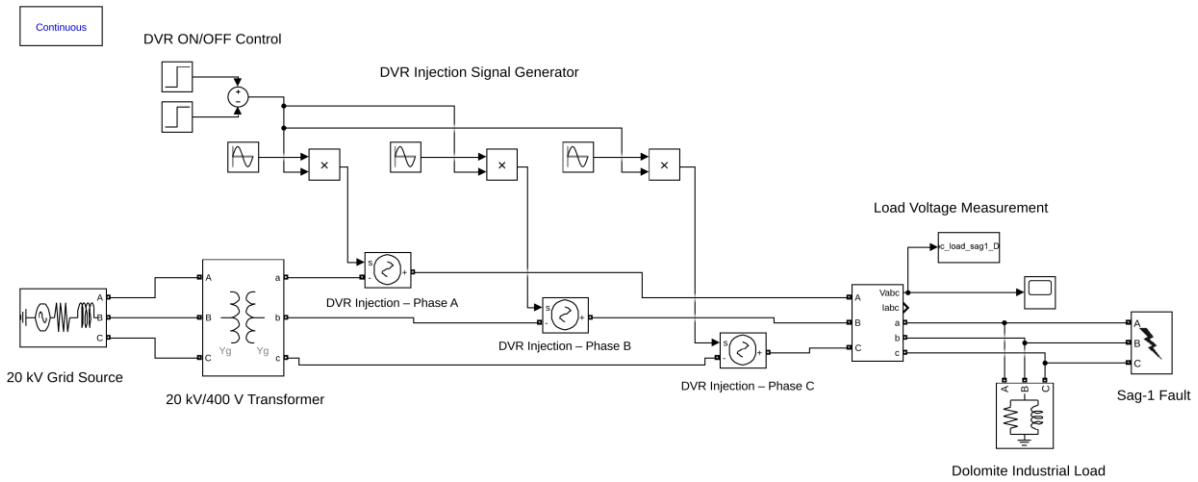


Figure 1. MATLAB/Simulink equivalent DVR model with three-phase series voltage injection

Performance Evaluation Method

All indicators were calculated from line-to-line rms voltages at the load terminal. The analytical compensation requirement was

$$V_{req} = V_{ref} - V_{sag} \quad (2)$$

where V_{req} is the required line-to-line rms compensation voltage, V_{ref} is the stabilized pre-sag reference, and V_{sag} is the uncompensated Sag-1 voltage. Disturbance severity was quantified by

$$Sag = \frac{V_{ref} - V_{sag}}{V_{ref}} \times 100 \quad (3)$$

$$V_{ret} = \frac{V_{sag}}{V_{ref}} \times 100 \quad (4)$$

where Sag is sag depth and V_{ret} is retained voltage, both in percent. DVR performance was evaluated using

$$Recovery = \frac{V_{after}}{V_{ref}} \times 100 \quad (5)$$

$$E_{mit} = \frac{V_{after} - V_{sag}}{V_{ref} - V_{sag}} \times 100 \quad (6)$$

$$Error = \frac{|V_{ref} - V_{after}|}{V_{ref}} \times 100 \quad (7)$$

where V_{after} is the compensated load voltage, E_{mit} is mitigation effectiveness, and Error is recovery error. Recovery measures the final voltage against the reference; mitigation effectiveness measures the restored fraction of the sag-induced loss; and recovery error measures the remaining absolute deviation. Precision values were used internally, while the principal tables and discussion report two-decimal results.

RESULTS AND DISCUSSION

Voltage Profile Without DVR

The stabilized line-to-line load voltage was 406.57 V rms. During Sag-1 without compensation it fell to 345.35 V rms, producing a 61.22-V loss. The retained voltage was 84.94 percent and the sag depth was 15.06 percent. The reduction persisted for 0.10 s, or five cycles, and occurred with comparable magnitudes and regular phase displacement in all three line-to-

line waveforms. Figure 2 shows the magnitude reduction between the fault boundaries without evidence of an unbalanced phase collapse.

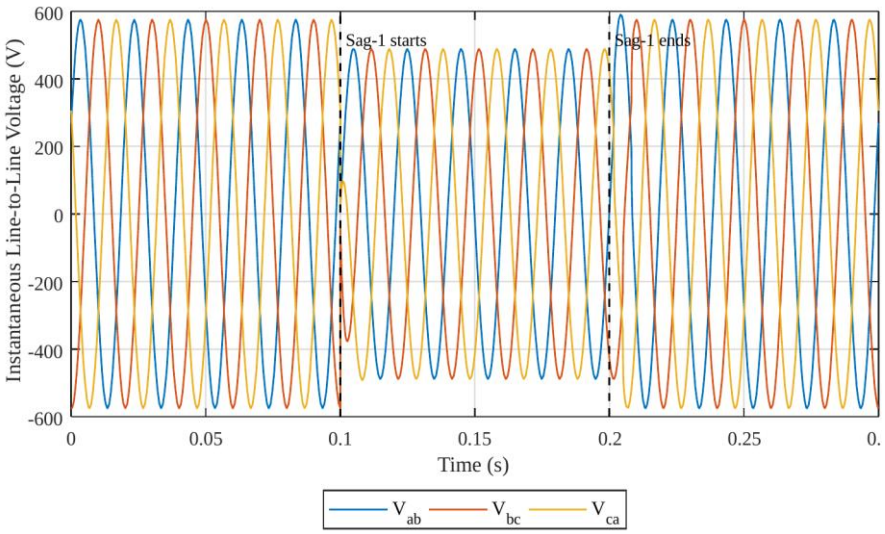


Figure 2. Instantaneous line-to-line voltage waveforms during Sag-1 without DVR compensation

Voltage Recovery With DVR

With the source, transformer, load, and fault parameters unchanged, the DVR raised the load voltage to 404.82 V rms during the same interval. The terminal increase from the uncompensated condition was 59.47 V, leaving a 1.75-V deficit relative to the 406.57-V reference. The compensated waveform remained sinusoidal and the three line-to-line voltages retained their ordered phase relationship, as shown in Figure 3. Because the recovered value remained below the reference, the selected injection did not produce overcompensation.

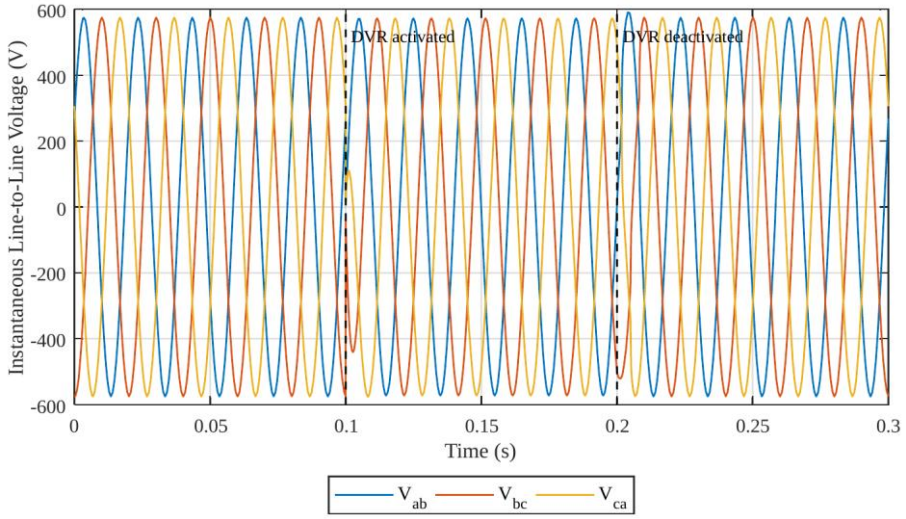


Figure 3. Instantaneous line-to-line voltage waveforms during Sag-1 with DVR compensation

Quantitative DVR Performance

Table 3. DVR performance evaluation results

Indicator	Result
Normal load voltage	406.57 V rms line-to-line
Sag-1 voltage without DVR	345.35 V rms line-to-line
Retained voltage	84.94 percent
Sag depth	15.06 percent
Required compensation	61.22 V rms line-to-line
Compensated voltage	404.82 V rms line-to-line
Restored terminal voltage	59.47 V rms line-to-line
Remaining deficit	1.75 V rms line-to-line
Voltage recovery	99.57 percent
Mitigation effectiveness	97.15 percent
Remaining uncompensated loss	2.85 percent
Recovery error	0.43 percent

The 99.57-percent recovery indicates that the compensated terminal voltage nearly reached its pre-sag value. The 97.15-percent mitigation effectiveness answers a different question: it shows that the DVR replaced 59.47 V of the 61.22-V sag-induced loss. Consequently, 2.85 percent of the original loss remained uncompensated, while the final recovery error relative to the reference was only 0.43 percent. Considering both indicators prevents a near-nominal final voltage from being misinterpreted as perfect compensation.

Technical Interpretation and Model Credibility

The 58-V peak-per-phase injection reference is an input to each controlled source. Its rms equivalent is 41.01 V per phase. Neither value is directly equal to the analytical 61.22-V line-to-line compensation requirement or to the simulated 59.47-V line-to-line terminal increase. The terminal result is formed through phase-domain series injection, phasor addition, and interaction with the source, transformer, and load impedances. This distinction is necessary to avoid a direct peak-to-rms or phase-to-line conversion that ignores the modeled network.

Model credibility was supported by six controls. The operating point was derived from actual AMR data; nonideal source and transformer parameters were included; the same load-

terminal measurement point and rms windows were used in every scenario; all base-system parameters were fixed between the uncompensated and compensated cases; the analytically required 61.22-V loss was consistent with the simulated 59.47-V restoration and 1.75-V residual; and the compensated three-phase waveforms remained balanced. These checks support the simulation-based performance evaluation without presenting the model as a complete switching-converter prototype.

The near-reference terminal recovery agrees with the established series-compensation behavior reported for medium-voltage DVR testing (Nielsen et al., 2004) and with industrial motor-load studies that evaluate performance at the protected terminal (El-Shennawy et al., 2010). It is also consistent with the principle that injection magnitude and phase must be coordinated with the disturbed voltage (Bhumkittipich & Mithulananthan, 2011). More generally, Rosyadi, Abduh, Kassim, et al. (2025) showed that inverter-based dynamic support must coordinate its output with the disturbed system variable to improve transient response; that frequency-stability application is conceptually relevant to response assessment but is not used here as evidence of DVR performance. In an electric-arc-furnace context, coordinated SVC–SWC compensation was evaluated through active/reactive-power response and terminal-voltage recovery (Rosyadi, Abduh, Widjaja, et al., 2025). Although the compensation mechanism differs from series DVR injection, that study supports the use of measured load-side recovery as a practical performance criterion.

At the evaluated point, the installation used 78.13 percent of its 555-kVA connected capacity, while the 630-kVA transformer carried 68.83 percent of its rating. The sag response was therefore evaluated at a substantial field-derived load without attributing the voltage reduction to transformer overload. The result is specific to the modeled feeder, operating point, balanced Sag-1 parameters, and equivalent DVR representation; it provides a contextual technical basis rather than a general claim for all PLN networks.

Suggestion for Future Research

Future research is expected to focus not only on enhancing voltage compensation capabilities but also on developing DVRs that are intelligent, adaptive, cost-effective, and reliable, while being integrated into Smart Grid and renewable energy ecosystems. Such an approach will enhance the resilience and reliability of power distribution systems in the face of increasing renewable energy penetration and the industry's growing demand for high power quality.

CONCLUSION

A balanced three-phase voltage sag (Sag-1) lasting 0.10 s reduced the root-mean-square (RMS) line-to-line voltage at the load terminals from 406.57 V to 345.35 V, corresponding to a retained voltage of 84.94% and a sag depth of 15.06%. The required voltage compensation was 61.22 V RMS line-to-line. Following equivalent three-phase dynamic voltage restorer (DVR) injection, the load-terminal voltage increased by 59.47 V to 404.82 V, leaving a residual voltage deficit of 1.75 V. The DVR achieved a voltage restoration level of 99.57% relative to the pre-sag voltage, a sag mitigation effectiveness of 97.15%, and a residual voltage error of 0.43%, without exceeding the pre-sag voltage level.

This study provided a simulation-based evaluation of DVR performance using field-derived operating data. Future research should incorporate laboratory experiments, hardware-

in-the-loop testing, and field validation to assess practical implementation. Further investigations should also consider detailed switching-level converter models, unbalanced and multiple voltage sag scenarios, techno-economic assessments, and integration with smart grid and renewable energy systems to strengthen the technical and economic feasibility of DVR deployment in utility-supplied medium-voltage distribution networks serving industrial facilities.

FUNDING

The authors declare that no financial support was received for the conduct of this research and/or the publication of this article.

CONFLICT OF INTEREST

The authors declare that this research was conducted in the absence of any commercial or financial relationships that could be construed as a potential conflict of interest.

AUTHOR CONTRIBUTIONS

All authors contributed to the preparation and writing of this article.

GENERATIVE AI STATEMENT

In the preparation of this manuscript, the authors utilized Artificial Intelligence (AI) solely for the purposes of improving grammar and checking language usage.

REFERENCES

Abdelaal, A. K., Shaheen, A. M., El-Fergany, A. A., & Alqahtani, M. H. (2024). Sliding mode control based dynamic voltage restorer for voltage sag compensation. *Results in Engineering*, *24*, 102936. https://doi.org/10.1016/j.rineng.2024.102936

Abdul Rahman, S., Kassahun, H. E., Tefera, B. A., Huluka, M. A., Belay, T. M., & Tarekegn, B. (2024). Voltage sag, swell, and interruption compensation using DVR based on energy storage device. *IEEE Access, 12*, 50834–50840. https://doi.org/10.1109/ACCESS.2024.3384876

Bhumkittipich, K., & Mithulananthan, N. (2011). Performance enhancement of DVR for mitigating voltage sag/swell using vector control strategy. *Energy Procedia*, *9*, 366–379. https://doi.org/10.1016/j.egypro.2011.09.040

Bollen, M. H. J. (2000). *Understanding power quality problems: Voltage sags and interruptions*. Wiley-IEEE Press.

Dugan, R. C., McGranaghan, M. F., Santoso, S., & Beaty, H. W. (2012). *Electrical power systems quality* (3rd ed.). McGraw-Hill.

El-Shennawy, T. I., Moussa, A., El-Gammal, M. A., & Abou-Ghazala, A. Y. (2010). A dynamic voltage restorer for voltage sag mitigation in a refinery with induction motors loads. *American Journal of Engineering and Applied Sciences*, *3*(1), 144–151. https://doi.org/10.3844/ajeassp.2010.144.151

Fuchs, E. F., & Masoum, M. A. S. (2023). *Power quality in power systems, electrical machines, and power-electronic drives* (3rd ed.). Academic Press.

Institute of Electrical and Electronics Engineers. (2023). *IEEE guide for economic loss evaluation of sensitive industrial customers caused by voltage sags* (IEEE Std 2938-2023). IEEE.

International Electrotechnical Commission. (2021). *Electromagnetic compatibility (EMC)—Part 4-30: Testing and measurement techniques—Power quality measurement methods* (IEC 61000-4-30:2015+AMD1:2021).

Liu, D., Zhang, H., Liang, X., & Deng, S. (2024). Model predictive control for three-phase, four-leg dynamic voltage restorer. *Energies, 17*(22), Article 5622. https://doi.org/10.3390/en17225622

Mattar, E.-Z. M., Mahmoud, E. S., & El-Sayed, M. I. (2024). Mitigation of voltage sag and voltage swell by using dynamic voltage restorer. *International Journal of Power Electronics and Drive Systems, 15*(2), 1290–1299. https://doi.org/10.11591/ijpeds.v15.i2.pp1290-1299

Mbuli, N. (2023). Dynamic voltage restorer as a solution to voltage problems in power systems: Focus on sags, swells and steady fluctuations. *Energies*, *16*(19), 6946. https://doi.org/10.3390/en16196946

Moghassemi, A., & Padmanaban, S. (2020). Dynamic voltage restorer (DVR): A comprehensive review of topologies, power converters, control methods, and modified configurations. *Energies*, *13*(16), 4152. https://doi.org/10.3390/en13164152

Nielsen, J. G., Newman, M., Nielsen, H., & Blaabjerg, F. (2004). Control and testing of a dynamic voltage restorer (DVR) at medium voltage level. *IEEE Transactions on Power Electronics*, *19*(3), 806–813. https://doi.org/10.1109/TPEL.2004.826504

Pilipenko, V. (2025). Analysis of causes and consequences of voltage sags in industrial power supply systems. *Information Technologies in Metallurgy and Machine Building*. https://doi.org/10.34185/1991-7848.itmm.2025.01.085

Prasad, D., Dhanamjayulu, C., & Stonier, A. A. (2022). A review of control techniques and energy storage for inverter-based dynamic voltage restorer in grid-integrated renewable sources. *Mathematical Problems in Engineering, 2022*, 1–43. https://doi.org/10.1155/2022/6389132

Rosyadi, M., Abduh, S., Kassim, M., Widjaja, R. E., & Hajar, I. (2025). Virtual inertia control for grid-connected wind farms: A novel approach to frequency stability enhancement. In *Proceedings of the 28th International Conference on Electrical Machines and Systems (ICEMS)*. https://doi.org/10.23919/ICEMS66262.2025.11317043

Rosyadi, M., Abduh, S., Widjaja, R. E., Rendroyoko, I., Hajar, I., & Soedibyo, B. A. (2025). Coordination of SVC and SWC control systems to enhancing power grid stability during disturbances caused by electric arc furnace. In *Proceedings of the International Conference on Advanced Technologies in Energy and Informatic (ICATEI)* (pp. 493–498). https://doi.org/10.1109/ICATEI67676.2025.11405211

Siddique, A., Mujahid, A., Aslam, W., Sajid, M., & Arfeen, Z. A. (2024). Improvements in voltage profile of JDW Sugar Mills' Jawar distribution feeder RYK Pakistan using ANN based dynamic voltage restorer. *Journal Européen des Systèmes Automatisés, 57*(1). https://doi.org/10.18280/jesa.570101

Soomro, A. H., Larik, A. S., Mahar, M. A., Sahito, A. A., Soomro, A. M., & Kaloi, G. S. (2021). Dynamic voltage restorer—A comprehensive review. *Energy Reports*, *7*, 6786–6805. https://doi.org/10.1016/j.egyr.2021.09.004

Tan, K.-H., Chen, J.-H., & Lee, Y.-D. (2023). Intelligent controlled dynamic voltage restorer for improving transient voltage quality. *IEEE Access*, *11*, 74686–74701. https://doi.org/10.1109/ACCESS.2023.3293823

Tang, L., Han, Y., Yang, P., Wang, C., & Zalhaf, A. S. (2022). A review of voltage sag control measures and equipment in power systems. *Energy Reports*, *8*(Suppl. 10), 207–216. https://doi.org/10.1016/j.egyr.2022.05.158

Wu, Z., Li, T., & Li, K. (2021). Experimental study on voltage sag tolerance of adjustable

speed drive with AC contactor. *2021 International Conference on Power System Technology (POWERCON)*, 1612–1616.